ACS Catalysis

Research Article

pubs.acs.org/acscatalysis

Mechanistic Insight into the Gold-Catalyzed Carboxylative Cyclization of Propargylamines

Ruming Yuan[†,‡] and Zhenyang Lin*[,†]

[†]Department of Chemistry, The Hong Kong University of Science and Technology, Clear Water Bay, Kowloon, Hong Kong, People's Republic of China

[‡]Department of Chemistry, Xiamen University, Xiamen 361005, People's Republic of China

Supporting Information

ABSTRACT: DFT calculations have been carried out to study the detailed mechanisms for the carboxylative cyclization of propargylamine using CO_2 catalyzed by NHC-gold(I) complexes. The calculation results indicate that the reaction starts with an N-coordinated species, [(NHC)-Au(propargylamine)]Cl, which undergoes isomerization to an alkyne-coordinated species. An amine−carbon dioxide interaction gives a carbamate ion species, from which a nucleophilic attack of the in-plane lone pair of electrons in the carbamate anion moiety on one of two coordinated alkyne carbons leads to formation of a five-membered-ring intermediate. The final product is generated through deprotonation and protonation processes. Through a detailed mechanistic study, we found that the substrate propargylamine assists (catalyzes) the deprotonation and protonation processes. Careful study of the solvent effect indicates that solvents, which are polar and capable of hydrogen bonding, promote the catalytic reactions through stabilizing the carbamate ion intermediate species.

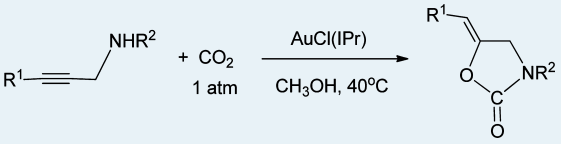

KEYWORDS: *carbon dioxide, propargylamines, gold(I) catalyst, carboxylative cyclization, DFT study*

INTRODUCTION

Carbon dioxide is an abundant, inexpensive and nontoxic renewable C1 building block.[1−3] The development of efficient catalytic processes for the transformation of carbon dioxide (CO_2) into desirable, economically competitive products is of great interest and has been a longstanding goal for chemists.[4,5] Recently, much effort has been made to develop chemical fixation of CO_2 into propargylamines to provide oxazolidinone derivatives.[6,7] The synthesis of oxazolidinone derivatives from the fixation of CO_2 has been considered as an attractive synthetic method.[7e,8]

Recently, it has been found that NHC-gold(I) complexes are able to catalyze carboxylative cyclization of propargylamines to afford oxazolidinone products in methanol in the absence of base additives under an atmospheric pressure of CO_2 at 40 °C with yields up to 91% (eq 1).[9] Experimental studies show that, when

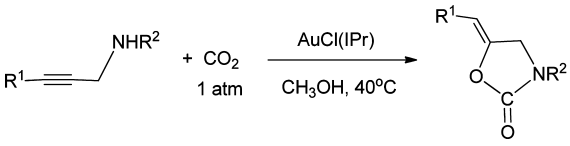

(1)

the catalytic reactions were carried out in weak polar solvents, such as THF, CH_2Cl_2, and toluene, no expected oxazolidinone products were produced. Furthermore, when the reactions were carried out in acetonitrile (CH_3CN), which is also a polar solvent and has a dielectric constant similar to that of methanol, the yields were unexpectedly as low as 15%. In eq 1, we can see that five-membered-ring, instead of six-membered-ring, products were experimentally observed.

In this work, we computationally study the detailed mechanism of the Au(I)-catalyzed carboxylative cyclization reactions shown in eq 1. Through detailed mechanistic studies, we hope to provide important insights into the reactions and to understand/explain the intriguing and interesting experimental observations regarding the choice of solvents and the regioselectivity mentioned above.

COMPUTATIONAL DETAILS

All quantum chemical calculations were performed using the hybrid density functional theory B3LYP.[10] In the B3LYP calculations, the gold atom is treated with the SDD relativistic effective core potential and the associated 6s5p3d valence basis set.[11] For O, N, and Cl, the 6-311+G(d) basis set was used, while the other atoms (C, H) were described by the standard 6-31G(d,p) basis set.[12,13] In addition, the polarizable continuum model (PCM) was chosen to account for the solvent effect and all the structures were fully optimized with PCM turned on.[14] Different solvents, such as CH_3OH, CH_3CN, CH_2Cl_2, THF, and toluene, were chosen in the PCM geometry optimizations. Important structures were visualized using the XYZviewer software developed by de Marothy.[15] Vibrational frequency calculations at the same level of theory were performed to verify that a local minimum has no imaginary frequency and each transition state has only one single imaginary frequency. Intrinsic reaction coordinate (IRC) calculations were also performed to

Received: February 6, 2015
Revised: March 23, 2015
Published: March 25, 2015

DOI: 10.1021/acscatal.5b00252
ACS Catal. 2015, 5, 2866−2872

make sure each transition state calculated indeed connects two relevant minima.[16] In addition, natural bond orbital (NBO) analyses were also performed using the NBO program as implemented in the Gaussian software packages.[17]

To obtain dispersion-corrected relative free energies, we performed single-point energy calculations for all of the species studied using B3LYP+D3/6-311++G(d,p)/PCM with the gold atom being still treated with the SDD basis set.[18] To reduce overestimation of the entropy contribution, we employed a correction of −2.6 (or 2.6) kcal/mol for 2:1 (or 1:2) transformations as many earlier theoretical studies did.[19] Unless specifically mentioned, dispersion- and entropy-corrected free energies in 298 K were used in all of our discussion in this article. All of the DFT calculations were carried out with the Gaussian 09 program.[20]

RESULTS AND DISCUSSION

According to the experimental results, a brief mechanism shown in Scheme 1 was proposed to account for the Au(I)-catalyzed carboxylative cyclization reactions shown in eq 1.[9] In the brief mechanism, it was considered that in a polar solvent such as methanol the chlorogold(I) precursor [AuCl] can ionize to form the active cationic species $[Au]^+$. The active cationic species $[Au]^+$ can then coordinate with a propargylic carbamate anion (**A**), which is formed from carboxylation of the propargylamine substrate followed by deprotonation, to give intermediate **B** through coordination of the alkyne moiety. From **B**, nucleophilic attack of the carbamate anion on the activated triple bond can generate an alkenyl-gold intermediate (**C**). Finally, from **C**, protonation takes place to give the expected oxazolidinone product.

Scheme 1. Brief Mechanism for the Gold-Catalyzed Carboxylative Cyclization Reactions of Propargylamines

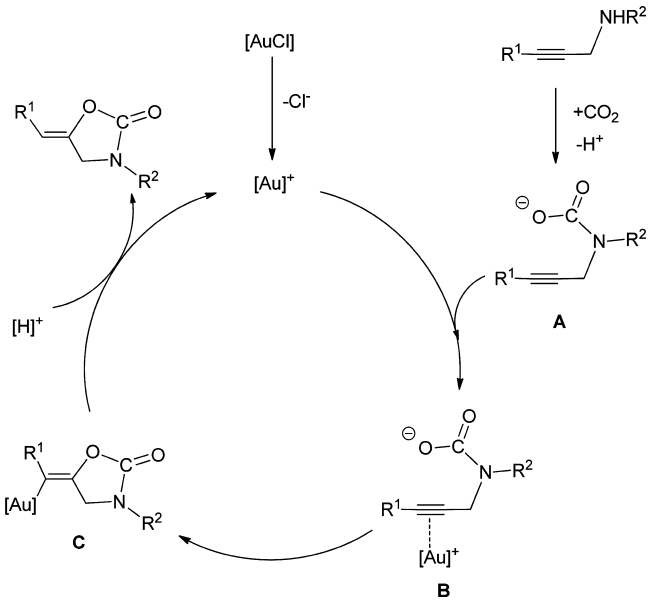

On the basis of the brief mechanism discussed above, we here provide a detailed mechanism to account for the carboxylative cyclization reactions, shown in Scheme 2, with 1-methylamino-2-butyne used as the representative propargylamine. The detailed mechanism shown in Scheme 2 takes into consideration of our calculation results, which will be discussed below.

Active Species for the Catalytic Reactions. Before we discuss the detailed reaction mechanism, it is necessary to discuss the active species involved on the basis of calculation results. In our DFT calculations, we used the experimentally employed 1-methylamino-2-butyne ($R^1 = R^2 = CH_3$) and IPr, respectively, as the representative propargylamine substrate molecule and the ligand. We first examined how easily the catalyst precursor (IPr)AuCl can be ionized in methanol to form $[(IPr)Au]^+$ and Cl^-. The ionization free energy calculated for (IPr)AuCl → $[(IPr)Au]^+ + Cl^-$ is 33.9 kcal/mol, which is too high for the ionization to occur.

Through our calculations, we found that a propargylamine substrate molecule easily interacts with the Au(I) metal center in (IPr)AuCl to form the N-coordinated species **1** (Scheme 2). With 1-methylamino-2-butyne as the propargylamine substrate molecule, the reaction free energy for (IPr)AuCl + propargylamine → **1** was calculated to be −3.3 kcal/mol. A linkage isomer of **1**, in which the Au(I) metal center coordinates with the alkyne moiety of 1-methylamino-2-butyne, was calculated to be less stable than **1** by 13.3 kcal/mol. These calculation results support that **1** is the likely active species to initiate the catalytic reactions (Scheme 2).

Energetics Associated with the Mechanism Shown in Scheme 2. After establishing the active species, we now examine the energetics associated with the mechanism starting from the active species **1** shown in Scheme 2. Figure 1 shows the free energy profiles calculated. Figure 2 gives the structures calculated for the relevant transition states related to the energy profiles shown in Figure 1.

From Figure 1, the first step is related to the isomerization from the N-coordinated species **1** to the alkyne-coordinated species **2** (a linkage isomer of **1**). The free energy barrier for this isomerization was calculated to be 19.7 kcal/mol, and as mentioned above, the alkyne-coordinated species **2** is less stable by 13.3 kcal/mol than the N-coordinated species **1**.

From the reactions shown in eq 1, the amine proton of a given propargylamine substrate migrates to one of the two alkyne carbons after the reaction. Therefore, deprotonation and protonation are expected to occur at a certain point. Our calculation results show that a propargylamine molecule assists/catalyzes the deprotonation process. From the alkyne-coordinated species **2**, a propargylamine molecule easily inserts via $\mathbf{TS}_{2\text{-}3}$ between the chloride anion and the alkyne-coordinated metal complex cation to form **3**. Then the amine N in **3** nucleophilically attacks the carbon center of an incoming CO_2 molecule to give **4**. The Cl^- ion associated with the species **3** makes the amine N more nucleophilic and promotes the transformation **3** + CO_2 → **4**. Finally, deprotonation occurs in **4**, giving the carbamate ion species **5** together with the ammonium salt $[(propargylamine)H]^+Cl^-$. Along the path for the transformation **2** + propargylamine + CO_2 → **5** + the ammonium salt, the highest energy transition state $\mathbf{TS}_{3\text{-}4}$ corresponds to the nucleophilic attack step and lies 20.5 kcal/mol above the reference energy point (Figure 1). For the transformation **2** + propargylamine + CO_2 → **5** + the ammonium salt, we also considered an alternative scenario in which the nucleophilic attack occurs prior to insertion of a propargylamine molecule. Our calculations show that this alternative scenario requires a higher overall barrier (by 4.6 kcal/mol) (see Figure S1 in the Supporting Information). Here, one may argue it is possible that the solvent methanol, instead of the substrate propargylamine, can also assist/catalyze the deprotonation process discussed above. We believe that this is less likely because methanol is a much weaker base than propargylamine. Additional calculations show that structures using methanol/methanol clusters to replace propargylamine

DOI: 10.1021/acscatal.5b00252
ACS Catal. 2015, 5, 2866−2872

Scheme 2. Detailed Mechanism for the Gold-Catalyzed Carboxylative Cyclization Reactions of Propargylamines[a]

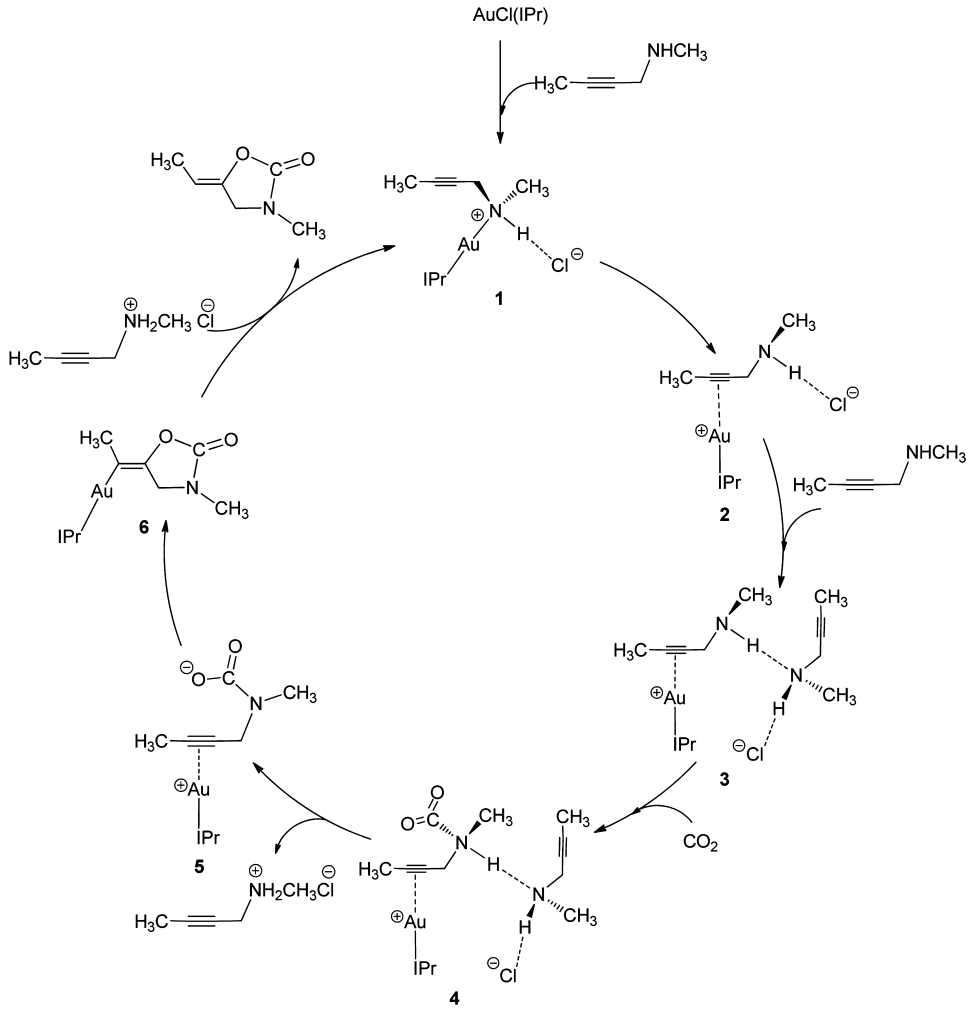

[a]Here, 1-methylamino-2-butyne is used as the representative propargylamine.

in **3** (Figure 1) are much less stable than **3** (see Figure S2 in the Supporting Information).

The next step is ring formation from the carbamate ion species **5**. Since the coordinated alkyne moiety contains two alkyne carbons, formation of either a five- or six-membered ring is possible. As shown in Figure 1b, formation of a five-membered ring (**6**) via $\mathbf{TS}_{5\text{-}6}$ is more favorable than formation of a 6-membered ring (7) via $\mathbf{TS}_{5\text{-}7}$. After carefully examining the two ring-formation transition state structures, we explain the regioselectivity of this ring formation step as follows. The five-membered-ring transition state structure shows good planarity in the five-membered ring. However, the six-membered ring in the transition state $\mathbf{TS}_{5\text{-}7}$ deviates from planarity significantly. It is expected that the ring formation process involves nucleophilic attack of the carbamate anion on an alkyne carbon, and the transition states $\mathbf{TS}_{5\text{-}6}$ and $\mathbf{TS}_{5\text{-}7}$ both make use of the lone pair of electrons, which occupy the in-plane p orbital of the attacking oxygen in the carbamate anion moiety, for the nucleophilic attack. The in-plane lone pair should be of higher nucleophilic reactivity than the π-bonding electron pairs in the carbamate anion moiety. Because of the good planarity, the five-membered-ring transition state $\mathbf{TS}_{5\text{-}6}$ can make good use of the in-plane lone pair of electrons. In contrast, because of the poor planarity, the six-membered-ring transition state $\mathbf{TS}_{5\text{-}7}$ cannot effectively make use of the in-plane lone pair of electrons for the nucleophilic attack, giving rise to a higher reaction barrier for the formation of the six-membered-ring intermediate **7** than the five-membered-ring intermediate **6**, though the two intermediates 7 and **6** show similar stability (Figure 1b).

The argument above indeed gains support from the second-order perturbation energy calculations within the NBO analysis. The second-order perturbation energies involving the aforementioned orbital interactions were estimated to be 14.2 kcal/mol for $\mathbf{TS}_{5\text{-}6}$ and 7.2 kcal/mol for $\mathbf{TS}_{5\text{-}7}$, indicating that the orbital interaction related to the nucleophilic attack in $\mathbf{TS}_{5\text{-}6}$ is indeed more effective than that in $\mathbf{TS}_{5\text{-}7}$.

After the formation of the favorable ring intermediate **6**, the final step is protonation to give the expected five-membered-ring oxazolidinone product. Here, the proton for the protonation comes from the ammonium salt formed from the deprotonation step. Our calculations show that the protonation step is very easy to occur (Figure 1b). Clearly, propargylamine acts as a catalyst for the deprotonation and protonation process.

As shown in Figure 1, the rate-determining transition state for the whole carboxylative cyclization reaction is $\mathbf{TS}_{5\text{-}6}$, which corresponds to the formation of the five-membered-ring intermediate **6**. The overall rate-determining free energy barrier was calculated to be 24.5 kcal/mol. The overall carboxylative

DOI: 10.1021/acscatal.5b00252
ACS Catal. 2015, 5, 2866−2872

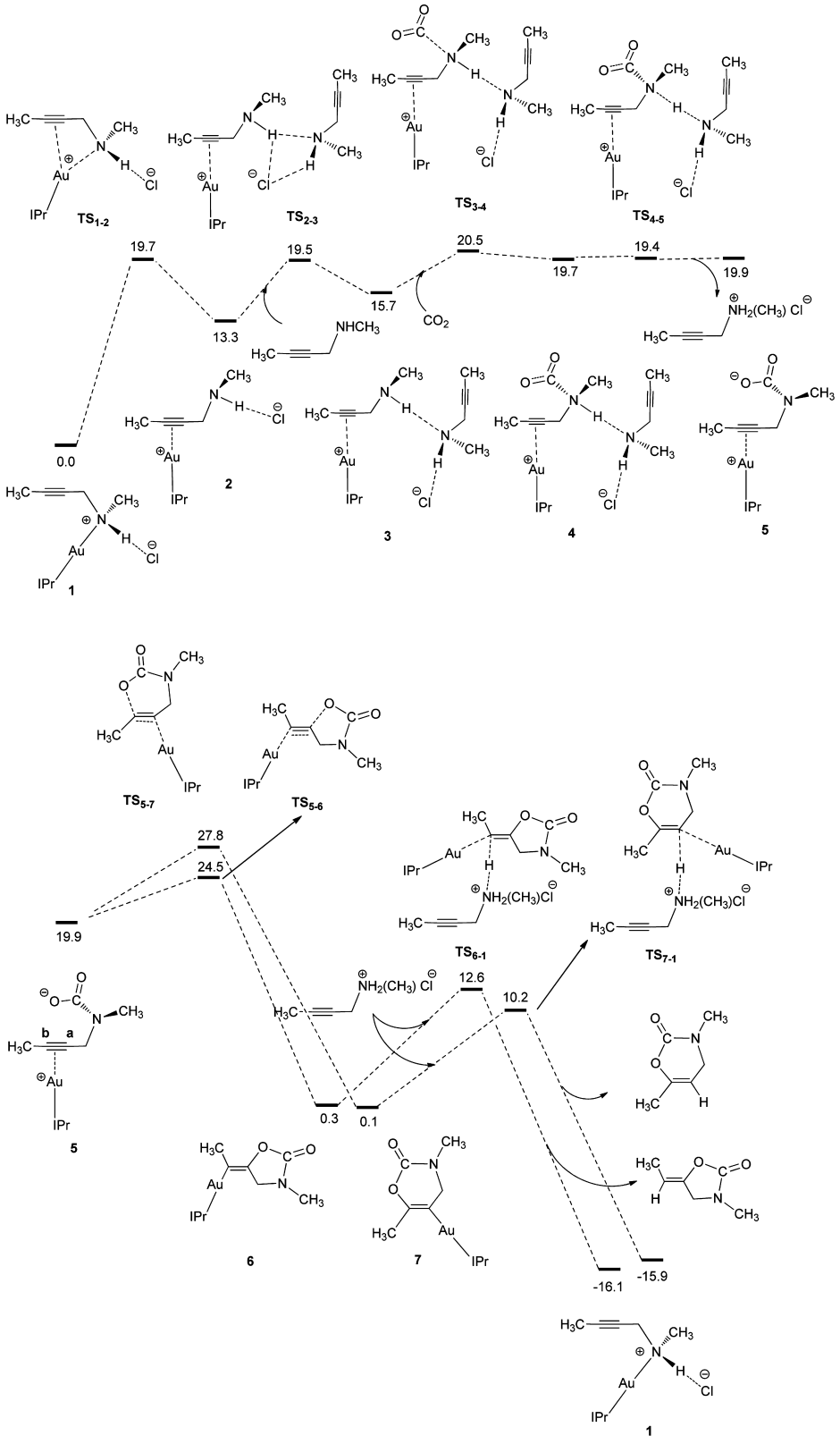

Figure 1. Free energy profiles calculated for the favorable pathway of the carboxylative cyclization reaction on the basis of Scheme 2. The free energies are given in kcal/mol. Methanol was used as the solvent in the PCM geometry and energy calculations.

cyclization reaction is exergonic by 16.1 kcal/mol, which is thermodynamically favorable.

Alternative Pathway Leading to Formation of 5 from 1. As shown in Scheme 3, from the N-coordinated species **1**, deprotonation can occur directly with the aid of a propargylamine molecule to first give **8**. Then isomerization of the amine N-coordinated species **8** to give an alkyne-coordinated species (**9**) takes place, followed by nucleophilic attack of the incoming

DOI: 10.1021/acscatal.5b00252
ACS Catal. 2015, 5, 2866−2872

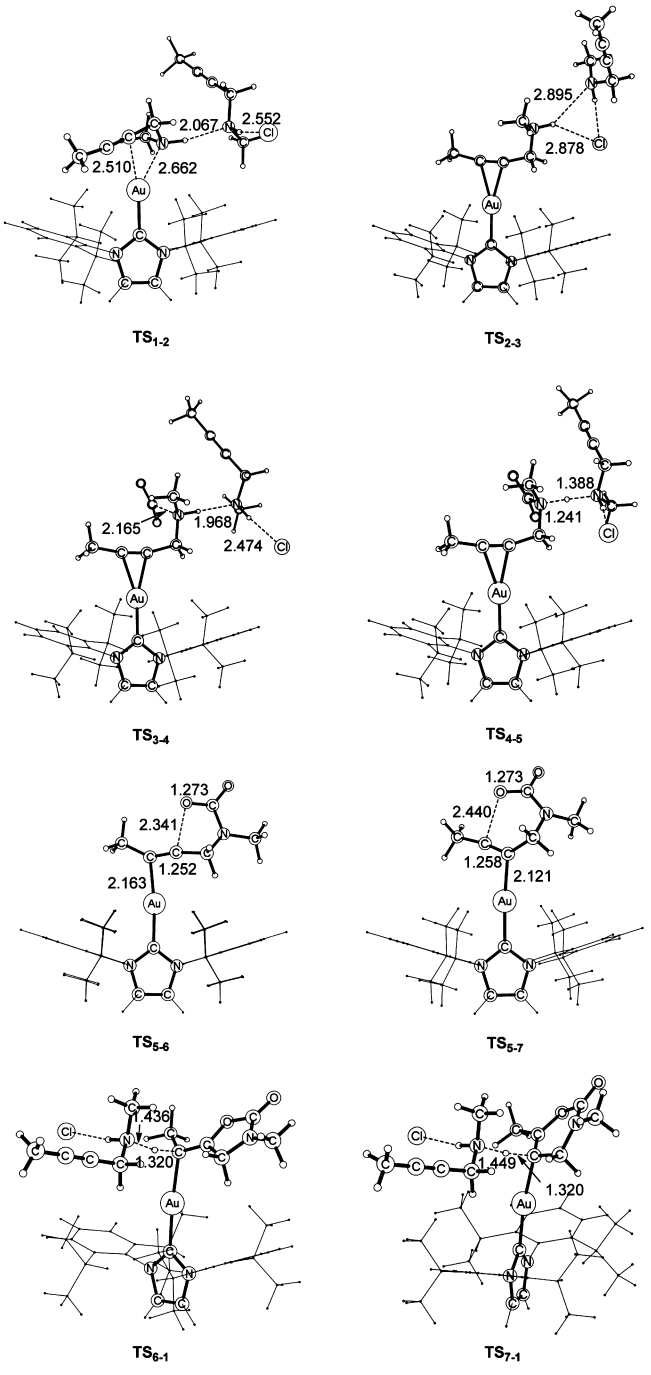

Figure 2. Calculated structures for relevant transition states along the energy profiles shown in Figure 1. Bond lengths are given in Å.

CO_2 carbon to give species **5**. Our calculation results show that the transformation of **1** + propargylamine → **8** + the ammonium salt is endergonic by 24.0 kcal/mol, which is thermodynamically very unfavorable. The barrier for the formation of **8** is expected to be higher than 24.0 kcal/mol. All of these results suggest that this alternative pathway is not responsible for the catalytic reactions studied.

Effect of Solvent. Through the detailed mechanistic discussion above, we have achieved an understanding of the regioselectivity observed experimentally. The other objective of this work is to understand why the polar solvent methanol (CH_3OH), not acetonitrile (CH_3CN), is effective for the catalytic reactions.

Experimentally, reactions carried out in weak polar solvents, such as THF, CH_2Cl_2, and toluene, resulted in no expected oxazolidinone products. It was also found that when the reaction was carried out in CH_3CN, which is a strongly polar solvent and has a dielectric constant similar to that of methanol, the yield was unexpectedly as low as 15%. In order to understand the effect of the solvents on the reaction outcomes, we calculated the ring formation (rate-determining) transition states $\mathbf{TS_{5\text{-}6}}$ and the carbamate ion species **5** in the solvents CH_3CN, CH_2Cl_2, THF, and toluene and compared their relative stabilities.

Table 1 shows the results of our calculations. In order for readers to better understand the relative polarity of the solvents, the dielectric constants of the solvents are also given in Table 1. In the table, we can clearly see that the more polar the solvent, the lower the ring formation transition state $\mathbf{TS_{5\text{-}6}}$, consistent with the experimental observation that weakly polar solvents do not promote the reactions. A plausible explanation is as follows. The stabilities of $\mathbf{TS_{5\text{-}6}}$ are closely related to the stabilities of the carbamate ion species **5** (Table 1). Clearly, the negatively charged dangling carboxylic group in **5** is significantly stabilized in a polar solvent, in turn lowering the energy of the transition state $\mathbf{TS_{5\text{-}6}}$. Table 1 also gives the results of our calculations for $\mathbf{TS_{5\text{-}7}}$ in different solvents. The stability trend in different solvents is similar to what we observed for $\mathbf{TS_{5\text{-}6}}$, and the five-membered-ring transition states $\mathbf{TS_{5\text{-}6}}$ always lie lower than the corresponding six-membered-ring transition states $\mathbf{TS_{5\text{-}7}}$.

Table 1. Relative Free Energies of the Carbamate Ion Species 5 + Ammonium Salt and the Ring Formation Transition States $\mathbf{TS_{5\text{-}6}}$ in Different Solvents

solvent	5 + [(propargylamine)H]$^+$Cl$^-$ (kcal/mol)	$\mathbf{TS_{5\text{-}6}}$ (kcal/mol)	$\mathbf{TS_{5\text{-}7}}$ (kcal/mol)	dielectric constant
CH_3OH	19.9	24.5	27.8	32.6
CH_3CN	18.8	23.4	26.7	35.7
CH_2Cl_2	22.2	25.4	28.6	8.9
THF	23.9	27.0	29.8	7.4
toluene	30.7	33.5	34.1	2.4

While the trend in the overall rate-determining barriers calculated for the nonpolar solvents CH_2Cl_2, THF, and toluene versus the polar solvents CH_3OH and CH_3CN was correctly

Scheme 3. Alternative Pathway Leading to Formation of 5

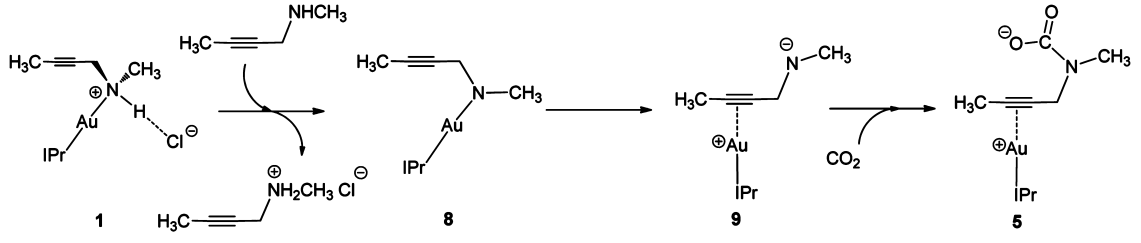

DOI: 10.1021/acscatal.5b00252
ACS Catal. 2015, 5, 2866−2872

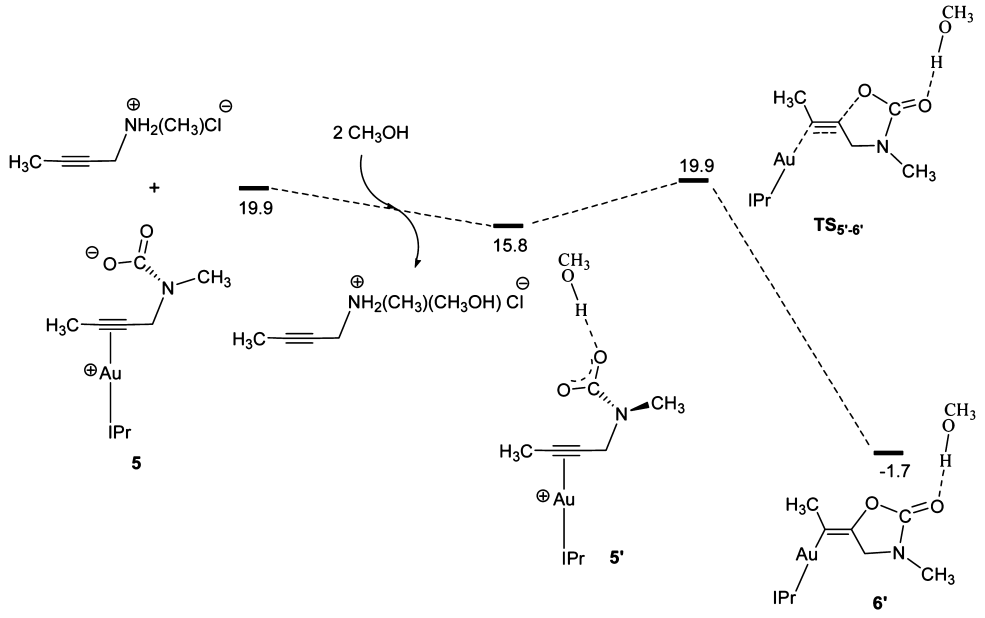

Figure 3. Free energy profiles calculated for the ring formation assisted by CH_3OH through hydrogen bonding. The free energies are given in kcal/mol. Methanol was used as the solvent in the PCM geometry and energy calculations.

predicted against the experimental observations, the trend calculated for the polar solvent CH_3OH versus CH_3CN was apparently not (Table 1). The overall rate-determining free energy barrier calculated for the CH_3OH solvent is higher than that calculated for the CH_3CN solvent, though the reaction yields in CH_3OH are much better than those in CH_3CN. To resolve this inconsistency between theory and experiment, we naturally think of the hydrogen-bonding capability of CH_3OH solvent molecules, which was not considered in the calculations up to this point. With this thinking, we found that CH_3OH can further stabilize the carbamate ion species **5** as well the transition state $\mathbf{TS_{5\text{-}6}}$ through hydrogen bonding. Our calculations (Figure 3) show that **5** and the ammonium salt each can be stabilized by one molecule of CH_3OH. Similarly, $\mathbf{TS_{5\text{-}6}}$ is also significantly stabilized by interacting with CH_3OH (from 24.5 to 19.9 kcal/mol). In other words, after taking into account the hydrogen-bonding capability of CH_3OH, we are able to explain the experimental observation that CH_3OH is a better solvent promoting the reactions than CH_3CN. Readers may have noticed that an ammonium salt was generated in the step of **4** to **5** (Figure 1). Thus, one may say that the ammonium salt can play the stabilizing role for the carbamate ion species **5** and the transition state $\mathbf{TS_{5\text{-}6}}$. We argue that, once generated, the ammonium salt is immediately consumed in the very facile protonation step that follows (Figure 1). The amount of the ammonium salt is very limited, and the protonation is fast and strongly thermodynamically driven (Figure 1). Therefore, we do not expect that the ammonium salt is involved in the role discussed above.

CONCLUSIONS

The detailed mechanisms for the carboxylative cyclization of propargylamine using CO_2 catalyzed by NHC-gold(I) complexes have been studied with the aid of DFT calculations. Scheme 2 summarizes the finding regarding the reaction mechanism.

The calculation results indicate that the reaction starts with an N-coordinated species, [(NHC)Au(propargylamine)]Cl, which undergoes isomerization to give an alkyne-coordinated species. From the alkyne-coordinated species, a propargylamine substrate molecule inserts between the chloride anion and the alkyne-coordinated complex cation, followed by a nucleophilic attack of the amine N on the carbon center of an incoming CO_2 molecule. Then deprotonation occurs aided by the inserted propargylamine molecule to give a carbamate ion species. Then, ring formation occurs in the carbamate ion species, which is the rate-determining step of the reaction. In the ring formation, both of the transition states leading to five- and six-membered rings involve a nucleophilic attack of the in-plane lone pair of electrons in the carbamate anion moiety on an alkyne carbon. The five-membered-ring transition state shows good planarity and makes good use of the in-plane lone pair of electrons for the nucleophilic attack, explaining the experimentally observed regioselectivity favoring the five-membered-ring product. Finally, protonation, accompanied by release of the inserted propargylamine molecule, occurs to give the expected five-membered-ring oxazolidinone product. Here, the substrate acts as a catalyst for the deprotonation and protonation process.

We also found that the negatively charged dangling carboxylic group in the carbamate ion species is significantly stabilized in a polar solvent, in turn lowering the energy of the rate-determining transition state. In addition, the hydrogen-bonding capability of the CH_3OH solvent molecules can further lower the energy of the rate-determining transition state, promoting the catalytic reactions.

ASSOCIATED CONTENT

Supporting Information

The following file is available free of charge on the ACS Publications website at DOI: 10.1021/acscatal.5b00252.

Energy profiles for the nucleophilic attack prior to insertion of a propargylamine molecule and the Cartesian coordinates and electronic energies for all of the calculated structures (PDF)

AUTHOR INFORMATION

Corresponding Author

*E-mail for Z.L.: chzlin@ust.hk.

DOI: 10.1021/acscatal.5b00252
ACS Catal. 2015, 5, 2866−2872

Notes

The authors declare no competing financial interest.

■ ACKNOWLEDGMENTS

This work was supported by the Research Grants Council of Hong Kong (GRF 16303614) and the National Natural Science Foundation of China (21203156).

■ REFERENCES

(1) (a) Marks, T. J. *Chem. Rev.* **2001**, *101*, 953−996. (b) Behr, A. *Angew. Chem., Int. Ed. Engl.* **1988**, *27*, 661−678. (c) Louie, J. *Curr. Org. Chem.* **2005**, *9*, 605−623. (d) Aresta, M.; Dibenedotto, A. *Dalton Trans.* **2007**, *28*, 2975−2992. (e) Baiker, A. *Appl. Organomet. Chem.* **2000**, *14*, 751−762.

(2) (a) Sakakura, T.; Choi, J. C.; Yasuda, H. *Chem. Rev.* **2007**, *107*, 2365−2387. (b) Sakakura, T.; Kohon, K. *Chem. Commun.* **2009**, 1312−1330. (c) Cokoja, M.; Bruckmeier, C.; Rieger, B.; Herrmann, W. A.; Kühn, F. E. *Angew. Chem., Int. Ed.* **2011**, *50*, 8510−8537. (d) Decortes, A.; Castilla, A. M.; Kleij, A. W. *Angew. Chem., Int. Ed.* **2010**, *49*, 9822−9837.

(3) (a) Yin, X.; Moss, J. R. *Coord. Chem. Rev.* **1999**, *181*, 27−59. (b) Riduan, S. N.; Zhang, Y. *Dalton Trans.* **2010**, *39*, 3347−3357. (c) Darensbourg, D. J. *Inorg. Chem.* **2010**, *49*, 10765−10780. (d) Zhang, L.; Cheng, J.; Ohishi, T.; Hou, Z. *Angew. Chem., Int. Ed.* **2010**, *49*, 8670−8673. (e) Yang, Z. Z.; Zhao, Y. N.; He, L. N. *RSC Adv.* **2011**, *1*, 545−567. (f) Ohishi, T.; Zhang, L.; Nishiura, M.; Hou, Z. *Angew. Chem., Int. Ed.* **2011**, *50*, 8114−8117. (g) Mansell, S. M.; Kaltsoyannis, N.; Arnold, P. L. *J. Am. Chem. Soc.* **2011**, *133*, 9036−9051. (h) Kumar, S.; Kumar, P.; Jain, S. L. *RSC Adv.* **2013**, *3*, 24013−24016. (i) Bontemps, S.; Sabo-Etienne, S. *Angew. Chem., Int. Ed.* **2013**, *52*, 10253−10255. (j) Zhang, Y.; Hanna, B. S.; Dineeen, A.; Williard, P. G.; Bernskoetter, W. H. *Organometallics* **2013**, *32*, 3969−3979. (k) Horn, B.; Limberg, C.; Herwig, C.; Braun, B. *Chem. Commun.* **2013**, *49*, 10923−10925.

(4) (a) Ukai, K.; Aoki, M.; Takaya, J.; Iwasawa, N. *J. Am. Chem. Soc.* **2006**, *128*, 8706−8715. (b) Takaya, J.; Tadami, S.; Ukai, K.; Iwasawa, N. *Org. Lett.* **2008**, *10*, 2697−2700. (c) Ohishi, T.; Nishiura, M.; Hou, Z. *Angew. Chem., Int. Ed.* **2008**, *47*, 5792−5795. (d) Yang, C. G.; He, C. *J. Am. Chem. Soc.* **2007**, *127*, 6966−6967.

(5) (a) Boogaerts, I. I. F.; Nolan, S. P. *Chem. Commun.* **2011**, *47*, 3021−3024. (b) Boogaerts, I. I. F.; Nolan, S. P. *J. Am. Chem. Soc.* **2010**, *132*, 8858−8859. (c) Huang, K.; Sun, C. L.; Shi, Z. J. *Chem. Soc. Rev.* **2011**, *40*, 2435−2452. (d) Yeung, C. S.; Dong, V. M. *J. Am. Chem. Soc.* **2008**, *130*, 7826−7827. (e) Kobayashi, K.; Kondo, Y. *Org. Lett.* **2009**, *11*, 2035−2037. (f) Williams, C. M.; Johnson, J. B.; Rovis, T. *J. Am. Chem. Soc.* **2008**, *130*, 14936−14937. (g) Correa, A.; Martín, R. *J. Am. Chem. Soc.* **2009**, *131*, 15974−15975. (h) Mizuno, H.; Takaya, J.; Iwasawa, N. *J. Am. Chem. Soc.* **2011**, *133*, 1251−1253. (i) Yu, D. Y.; Zhang, Y. G. *Green Chem.* **2011**, *13*, 1275−1279. (j) Saito, S.; Nakagawa, S.; Koizumi, T.; Hirayama, K.; Yamamoto, Y. *J. Org. Chem.* **1999**, *64*, 3975−3978. (k) Shimizu, K.; Takimoto, M.; Sato, Y.; Mori, M. *Org. Lett.* **2005**, *7*, 195−197. (l) Aoki, M.; Kaneko, M.; Izumi, S.; Ukai, K.; Iwasawa, N. *Chem. Commun.* **2004**, 2568−2569.

(6) (a) Dimroth, P.; Pasedach, H. DE Pat. 1164411, 1964. (b) Dimroth, P.; Pasedach, H. *Chem. Abstr.* **1964**, *60*, 14510. (c) Mitsudo, T.; Hori, Y.; Yamakawa, Y.; Watanabe, Y. *Tetrahedron Lett.* **1987**, *28*, 4417−4418. (d) Bacchi, A.; Chiusoli, G. P.; Costa, M.; Gabriele, B.; Righi, C.; Salerno, G. *Chem. Commun.* **1997**, 1209−1210. (e) Shi, M.; Shen, Y.-M. *J. Org. Chem.* **2002**, *67*, 16−21. (f) Costa, M.; Chiusoli, G. P.; Taffurelli, D.; Dalmonego, G. *J. Chem. Soc., Perkin Trans. 1* **1998**, 1541−1546. (g) Yoshida, M.; Komatsuzaki, Y.; Ihara, M. *Org. Lett.* **2008**, *10*, 2083−2086. (h) Feroci, M.; Orsini, M.; Sotgiu, G.; Rossi, L.; Inesi, A. *J. Org. Chem.* **2005**, *70*, 7795−7798. (i) Maggi, R.; Bertolotti, C.; Orlandini, E.; Oro, C.; Sartori, G.; Selva, M. *Tetrahedron Lett.* **2007**, *48*, 2131−2134. (j) Kayaki, Y.; Yamamoto, M.; Suzuki, T.; Ikariya, T. *Green Chem.* **2006**, *8*, 1019−1021. (k) Costa, M.; Chiusoli, G. P.; Rizzardi, M. *Chem. Commun.* **1996**, 1699−1700.

(7) (a) Yamada, W.; Sugawara, Y.; Cheng, H.-M.; Ikeno, T.; Yamada, T. *Eur. J. Org. Chem.* **2007**, 2604−2607. (b) Yoshida, S.; Fukui, K.; Kikuchi, S.; Yamada, T. *J. Am. Chem. Soc.* **2010**, *132*, 4072−4073. (c) Yoshida, S.; Fukui, K.; Kikuchi, S.; Yamada, T. *Chem. Lett.* **2009**, *38*, 786−787. (d) Kikuchi, S.; Sekine, K.; Ishida, T.; Yamada, T. *Angew. Chem., Int. Ed.* **2012**, *51*, 6989−6992. (e) Kikuchi, S.; Yoshida, S.; Sugawara, Y.; Yamada, W.; Cheng, H.-M.; Fukui, K.; Sekine, K.; Iwakura, I.; Ikeno, T.; Yamada, T. *Bull. Chem. Soc. Jpn.* **2011**, *84*, 698−717. (f) Ishida, T.; Kikuchi, S.; Tsubo, T.; Yamada, T. *Org. Lett.* **2013**, *15*, 848−851.

(8) Visser, C. M.; Kellogg, R. M. *Bioorg. Chem.* **1977**, *6*, 79−88.

(9) Hase, S.; Kayaki, Y.; Ikariya, T. *Organometallics* **2013**, *32*, 5285−5288.

(10) (a) Vosko, S. H.; Wilk, L.; Nusair, M. *Can. J. Phys.* **1980**, *58*, 1200−1211. (b) Becke, A. D. *J. Chem. Phys.* **1993**, *98*, 5648−5652. (c) Lee, C. T.; Yang, W. T.; Parr, R. G. *Phys. Rev. B: Condens. Matter Mater. Phys.* **1988**, *37*, 785−787.

(11) (a) Fang, R.; Su, C.-Y.; Zhao, C.; Phillips, D. L. *Organometallics* **2009**, *28*, 741−748. (b) Biswas, S.; Dahlstrand, C.; Watile, R. A.; Kalek, M.; Himo, F.; Samec, J. S. M. *Chem. - Eur. J.* **2013**, *19*, 17939−17950.

(12) (a) McGrath, M. P.; Radom, L. *J. Chem. Phys.* **1991**, *94*, 511−516. (b) Raghavachari, K.; Binkley, J. S.; Seeger, R.; Pople, J. A. *J. Chem. Phys.* **1980**, *72*, 650−654.

(13) (a) Petersson, G. A.; Bennett, A.; Tensfeldt, T. G.; Al-Laham, M. A.; Shirley, W. A.; Mantzaris, J. *J. Chem. Phys.* **1988**, *89*, 2193−2218. (b) Petersson, G. A.; Al-Laham, M. A. *J. Chem. Phys.* **1991**, *94*, 6081−6090.

(14) Tomasi, J.; Mennucci, B.; Cammi, R. *Chem. Rev.* **2005**, *105*, 2999−3093.

(15) De Marothy, S. A. *XYZViewer version 0.97*; Stockholm, 2010.

(16) (a) Fukui, K. *J. Phys. Chem.* **1970**, *74*, 4161−4163. (b) Fukui, K. *Acc. Chem. Res.* **1981**, *14*, 363−368.

(17) (a) Reed, A. E.; Weinhold, F. *J. Chem. Phys.* **1983**, *78*, 4066−4073. (b) Reed, A. E.; Weinstock, R. B.; Weinhold, F. *J. Chem. Phys.* **1985**, *83*, 735−746. (c) Reed, A. E.; Weinhold, F. *J. Chem. Phys.* **1985**, *83*, 1736−1740. (d) Reed, A. E.; Curtiss, L. A.; Weinhold, F. *Chem. Rev.* **1988**, *88*, 899−926. (e) Carpenter, J. E.; Weinhold, F. *J. Mol. Struct.: THEOCHEM* **1988**, *46*, 41−62. (f) Foster, J. P.; Weinhold, F. *J. Am. Chem. Soc.* **1980**, *102*, 7211−7218.

(18) Grimme, S.; Ehrlich, S.; Goerigk, L. *J. Comput. Chem.* **2011**, *32*, 1456−1465.

(19) (a) Benson, S. W. *The Foundations of Chemical Kinetics*; Krieger: Malabar, FL, 1982. (b) Okuno, Y. *Chem. - Eur. J.* **1997**, *3*, 212−218. (c) Ardura, D.; López, R.; Sordo, T. L. *J. Phys. Chem. B* **2005**, *109*, 23618−23623. (d) Schoenebeck, F.; Houk, K. N. *J. Am. Chem. Soc.* **2010**, *132*, 2496−2497. (e) Liu, Q.; Lan, Y.; Liu, J.; Li, G.; Wu, Y. D.; Lei, A. *J. Am. Chem. Soc.* **2009**, *131*, 10201−10210. (f) Ariafard, A.; Brookes, N. J.; Stanger, R.; Yates, B. F. *Organometallics* **2011**, *30*, 1340−1349. (g) Yu, H.; Lu, Q.; Dang, Z.; Fu, Y. *Chem. - Asian J.* **2013**, *8*, 8−18. (h) Ariafard, A.; Ghohe, N. M.; Abbasi, K. K.; Canty, A. J.; Yates, B. F. *Inorg. Chem.* **2013**, *52*, 707−717. (i) Fan, T.; Sheong, F. K.; Lin, Z. *Organometallics* **2013**, *32*, 5224−5230. (j) Xie, H.; Lin, Z. *Organometallics* **2014**, *33*, 892−897. (k) Yuan, R.; Lin, Z. *ACS Catal.* **2014**, *4*, 4466−4473. (l) Yuan, R.; Lin, Z. *Organometallics* **2014**, *33*, 7147−7156.

(20) Frisch, M. J.; Trucks, G. W.; Schlegel, H. B.; Scuseria, G. E.; Robb, M. A.; Cheeseman, J. R.; Scalmani, G.; Barone, V.; Mennucci, B.; Petersson, G. A.; Nakatsuji, H.; Caricato, M.; Li, X.; Hratchian, H. P.; Izmaylov, A. F.; Bloino, J.; Zheng, G.; Sonnenberg, J. L.; Hada, M.; Ehara, M.; Toyota, K.; Fukuda, R.; Hasegawa, J.; Ishida, M.; Nakajima, T.; Honda, Y.; Kitao, O.; Nakai, H.; Vreven, T.; Montgomery, J. A., Jr.; Peralta, J. E.; Ogliaro, F.; Bearpark, M.; Heyd, J. J.; Brothers, E.; Kudin, K. N.; Staroverov, V. N.; Kobayashi, R.; Normand, J.; Raghavachari, K.; Rendell, A.; Burant, J. C.; Iyengar, S. S.; Tomasi, J.; Cossi, M.; Rega, N.; Millam, J. M.; Klene, M.; Knox, J. E.; Cross, J. B.; Bakken, V.; Adamo, C.; Jaramillo, J.; Gomperts, R.; Stratmann, R. E.; Yazyev, O.; Austin, A. J.; Cammi, R.; Pomelli, C.; Ochterski, J. W.; Martin, R. L.; Morokuma, K.; Zakrzewski, V. G.; Voth, G. A.; Salvador, P.; Dannenberg, J. J.; Dapprich, S.; Daniels, A. D.; Farkas, Ö.; Foresman, J. B.; Ortiz, J. V.; Cioslowski, J.; Fox, D. J. *Gaussian 09, Revision D.01*; Gaussian, Inc., Wallingford, CT, 2009.

DOI: 10.1021/acscatal.5b00252
ACS Catal. 2015, 5, 2866−2872